



# Effects of maleated polypropylene content on the extended creep behavior of wood–polypropylene composites using the stepped isothermal method and the stepped isostress method

Chung-Wei Huang<sup>1</sup> · Teng-Chun Yang<sup>1</sup> · Tung-Lin Wu<sup>1</sup> · Ke-Chang Hung<sup>1</sup> · Jyh-Horng Wu<sup>1</sup>

Received: 21 November 2017  
© Springer-Verlag GmbH Germany, part of Springer Nature 2018

## Abstract

This study investigated the effectiveness of maleated polypropylene (MAPP) as a coupling agent for improving the physico-mechanical properties and creep resistances of wood–polypropylene composites (WPCs). The results revealed that the composites with MAPP showed significantly decreased water absorption and thickness swelling, while the flexural properties and the wood screw holding strength increased as the MAPP content increased up to 3 wt%. Additionally, flexural creep tests were conducted at a series of elevated temperatures and stresses using the stepped isothermal method (SIM) and the stepped isostress method (SSM), respectively. The SSM-predicted creep compliance curves fit better with the experimental data than the SIM-predicted curves. On the other hand, the creep master curves for all of the WPCs were constructed from different SSM test conditions and were highly consistent with the long-term experimental creep data. The creep resistance values of the composites with MAPP were greater than those without MAPP, especially for the WPC with 5 wt% MAPP (WPC<sub>M5</sub>), due to the improvement in the interfacial compatibility between the wood fibers and PP matrix. Furthermore, according to the SSM-predicted creep behavior, the improvement in creep resistance (ICR) of WPC<sub>M5</sub> reached 61% over a 20-year period compared to the WPC without MAPP.

---

Chung-Wei Huang and Teng-Chun Yang have contributed equally to this work.

---

✉ Jyh-Horng Wu  
eric@nchu.edu.tw

<sup>1</sup> Department of Forestry, National Chung Hsing University, Taichung 402, Taiwan

## Introduction

In recent years, biocomposites reinforced with natural fibers (NFs) have been of significant interest and have attracted great attention as alternative materials instead of synthetic fibers since NFs have numerous significant advantages, such as low density, high toughness, good specific strength, renewability, and biodegradability (Xu et al. 2001; Zhang et al. 2002; Oksman et al. 2003; Saba et al. 2015). These characteristics of NFs can mitigate the drawbacks of the polymer matrix, which resulted in several advantages for polymer composites (Schneider et al. 2003; Klyosov 2007; Lee et al. 2010; Kumar et al. 2011; Dittenber and Ganga Rao 2012). Therefore, NFs can be used to make polymer composites into eco-friendly biomaterials and reduce the cost of the final products as well as serve as an alternative to synthetic fibers. However, the major drawbacks of hygroscopicity and incompatibility between the hydrophilic lignocellulosics and hydrophobic thermoplastics have been found to limit the applicability of wood-plastic composites (WPCs). Therefore, several physical and chemical approaches, such as esterification, alkaline treatment, and the addition of coupling agents, have been used to increase the hydrophobicity of lignocellulosic materials and improve their dimensional and thermal stabilities (Rowell 1983; Keener et al. 2004; Li et al. 2007; Das and Chakraborty 2008; Hung and Wu 2010; Pelaez-Samaniego et al. 2013). A small amount of coupling agent can be added to create bonds between the wood fibers (WFs) and polymer matrix and to improve the interphase compatibility in composites. The agent acts as a chemical bridge that links the reinforcement and the matrix. Copolymers containing maleic anhydride, such as maleated polypropylene (MAPP), are among the organic coupling agents commonly and widely used in WPCs. The maleic anhydrides of the copolymers entangle and cohere with the polymer matrix due to their similar polarities, and the other end of anhydride molecules can react to form covalent bonds with hydroxyl groups of the WF. After this treatment, the surface energy of the polypropylene (PP) matrix is much closer to that of the WF, resulting in better wettability and interfacial interactions with the PP matrix (Felix and Gatenholm 1991; Li et al. 2007; Ou et al. 2010). Several studies have reported that the use of MAPP as a coupling agent is an efficient approach for improving dimensional stability, mechanical properties, and impact strength (Mishra et al. 2000; Qiu et al. 2003; Mohanty et al. 2004; Bledzki et al. 2005).

Furthermore, WPCs are susceptible to time-dependent deformation when subjected to loading over an extended period due to the viscoelastic nature of the polymer matrix, which causes an increase in creep compliance of the composite. In engineering applications, the estimation of creep behavior is indispensable for the material design related to the load-bearing capacity of products. However, long-term creep tests conducted over a normal time scale are time-consuming and prohibitively expensive. Therefore, an accelerated creep test must be used to obtain the master curve, which is then fitted with an empirical mathematical model. The concept of the accelerated creep test for the prediction of the long-term performance is to use the superposition principle from the combination of exposure

time, exposure temperature, and applied load. Several studies (Dasappa et al. 2009; Hung et al. 2015; Yang et al. 2015) have reported that the creep behavior of viscoelastic materials using the time–temperature superposition principle (TTSP) can be determined from the stepped temperature in the same way as time equivalence. From this principle, the stepped isothermal method (SIM) has been developed to use stepped increments of temperature for a single sample (Jones and Clarke 2007; Alwis and Burgoyne 2008; Yeo and Hsuan 2010; Achereiner et al. 2013). Recently, several studies have used the stepped isostress method (SSM) approach to capture the creep behavior of a single sample with the step-wise increase in the stress level. This method was very successful in predicting the long-term creep behavior of various materials (Giannopoulos and Burgoyne 2011, 2012; Hadid et al. 2004, 2014; Tanks et al. 2017), such as semicrystalline thermoplastics and carbon fiber-reinforced polymer. However, little information is available regarding the effect of MAPP on the creep behavior of WPCs. Therefore, in addition to qualification of the physical properties and static mechanical properties of these materials, the present study investigated the time–temperature-dependent and time–stress-dependent behavior for extended creep behavior of WPCs with different MAPP contents using the SIM and SSM, respectively.

## Materials and methods

### Materials

WFs were prepared from a 52-year-old China fir (*Cunninghamia lanceolata*), which was kindly provided by the experimental forest of National Chung Hsing University (Nantou, Taiwan), via hammer-milling and sieving to obtain WFs between 16 and 24 mesh ( $\phi$ 1.00–0.71 mm). PP pellets (Globalene 7633) with a density of 896 kg/m<sup>3</sup>, melting point of 170 °C, and melt index of 2 g/10 min were purchased from LCY Chemical Co. (Taipei, Taiwan). Commercially available MAPP (maleic anhydride 8–10 wt%) for use as a coupling agent was purchased from Sigma-Aldrich Chemical Co. (St. Louis, MO, USA), and its density, melting point, and melt flow index were 934 kg/m<sup>3</sup>, 156 °C, and 115 g/10 min, respectively.

### Preparation of the composite panel

WPCs with various MAPP contents were compounded at 200 °C for 5 min by a YKI-3 Banbury mixer (Goldspring Enterprise Inc., Taichung, Taiwan) at a rotor speed of 50 rpm. As shown in Table 1, the weight ratios of oven-dried WF, PP, and MAPP were 60/40/0, 60/39/1, 60/37/3, 60/35/5, and 60/33/7 (wt%), respectively. The expected density of each WPC was 1000 kg/m<sup>3</sup>. After compounding, the mixtures were extruded and pelleted, and 12-mm-thick plate samples were hot-pressed at 180 °C and 2.5 MPa, then quenched to room temperature. In this study, the samples of WPCs with MAPP contents of 0, 1, 3, 5, and 7 wt% are designated as WPC<sub>0</sub>, WPC<sub>M1</sub>, WPC<sub>M3</sub>, WPC<sub>M5</sub>, and WPC<sub>M7</sub>, respectively.

**Table 1** Effects of MAPP content on the physico-mechanical properties of various WPCs

Code	WFs (wt%)	PP (wt%)	MAPP (wt%)	Density (kg/m <sup>3</sup> )	Moisture content (%)	24-h soaking		Flexural properties		Wood screw holding strength (kN)	Impact strength (kJ/m <sup>2</sup> )
						Water absorption (%)	Thickness swelling (%)	MOR (MPa)	MOE (GPa)		
WPC <sub>0</sub>	60	40	0	1069 ± 13 <sup>a</sup>	1.1 ± 0.3 <sup>a</sup>	1.1 ± 0.1 <sup>a</sup>	0.7 ± 0.3 <sup>a</sup>	16.8 ± 0.5 <sup>d</sup>	2.5 ± 0.1 <sup>b</sup>	1.1 ± 0.1 <sup>b</sup>	3.7 ± 0.1 <sup>a</sup>
WPC <sub>M1</sub>	60	39	1	1017 ± 41 <sup>a</sup>	1.4 ± 0.4 <sup>a</sup>	1.1 ± 0.1 <sup>a</sup>	0.4 ± 0.1 <sup>ab</sup>	27.6 ± 0.6 <sup>c</sup>	2.6 ± 0.1 <sup>b</sup>	1.8 ± 0.1 <sup>a</sup>	4.1 ± 0.4 <sup>a</sup>
WPC <sub>M3</sub>	60	37	3	1046 ± 20 <sup>a</sup>	1.0 ± 0.1 <sup>a</sup>	0.8 ± 0.0 <sup>b</sup>	0.4 ± 0.1 <sup>ab</sup>	33.5 ± 0.7 <sup>a</sup>	3.1 ± 0.1 <sup>a</sup>	2.0 ± 0.1 <sup>a</sup>	4.1 ± 0.2 <sup>a</sup>
WPC <sub>M5</sub>	60	35	5	1041 ± 29 <sup>a</sup>	1.2 ± 0.3 <sup>a</sup>	0.8 ± 0.0 <sup>b</sup>	0.2 ± 0.1 <sup>b</sup>	32.0 ± 0.7 <sup>a</sup>	3.3 ± 0.1 <sup>a</sup>	1.9 ± 0.1 <sup>a</sup>	3.8 ± 0.0 <sup>a</sup>
WPC <sub>M7</sub>	60	33	7	1066 ± 19 <sup>a</sup>	1.1 ± 0.1 <sup>a</sup>	0.8 ± 0.1 <sup>b</sup>	0.3 ± 0.1 <sup>b</sup>	30.0 ± 1.1 <sup>b</sup>	3.2 ± 0.1 <sup>a</sup>	1.9 ± 0.2 <sup>a</sup>	3.8 ± 0.5 <sup>a</sup>

Values are the mean ± SD (*n* = 5). Different letters within a column indicate significant differences (*p* < 0.05)

## Determining the composite properties

The physico-mechanical properties, including density, amount of water absorption, thickness swelling, flexural properties, and wood screw holding strength, were determined according to the Chinese National Standard CNS 2215. The modulus of rupture (MOR) and modulus of elasticity (MOE) data were obtained from samples with dimensions of 230 mm × 50 mm × 12 mm using a three-point static bending test at a loading speed of 10 mm/min and a span of 180 mm. The wood screw holding strength was determined (sample size 50 mm × 50 mm × 12 mm) at a tensile speed of 2 mm/min. In addition, the Charpy impact strength of notched samples was measured using a Yasuda 258 impact pendulum tester (Hyogo, Japan) according to ASTM D6110. All samples were conditioned at 20 °C and 65% relative humidity (RH) for 2 weeks prior to testing, and five samples of each WPC were tested.

## Accelerated and experimental creep tests

The stepped isothermal method (SIM) and stepped isostress method (SSM) were implemented using a universal testing machine (Shimadzu AG-10kNX, Tokyo, Japan) equipped with thermostatic chamber (Shimadzu TCE-N300KIT, Tokyo, Japan) to predict the long-term creep behavior of WPCs. According to the SIM, the creep strain at a reference temperature is given by the following equation (Eq. 1):

$$\varepsilon(T_r, t) = \varepsilon(T, t/\alpha_T) \quad (1)$$

where  $\varepsilon$  is the creep strain as a function of temperature and time,  $T_r$  is the reference temperature,  $T$  is the elevated temperature, and  $\alpha_T$  is the shift factor in the SIM. In addition, the William–Landel–Ferry (WLF) equation was used for the shift factor. The glass transition temperatures ( $T_g$ ) of WPC<sub>0</sub>, WPC<sub>M1</sub>, WPC<sub>M3</sub>, WPC<sub>M5</sub>, and WPC<sub>M7</sub> are determined as 17.3, 14.3, 13.7, 13.1, and 14.0 °C, respectively, by the differential scanning calorimeter (DSC) method. Therefore, the William–Landel–Ferry (WLF) equation was appropriately used for the shift factor because samples were tested at working temperatures in the range of  $T_g$  to  $T_g + 100$  °C (Liu et al. 2008). The shift factor, which is related to temperature, is calculated using the following equations (Eqs. 2–4):

$$\log \alpha_T = \frac{-C_1(T - T_{ref})}{(C_2 + T - T_{ref})} \quad (2)$$

$$C_1 = \frac{C_{1g}C_{2g}}{(C_{2g} + T_{ref} - T_g)} \quad (3)$$

$$C_2 = C_{2g} + T_{ref} - T_g \quad (4)$$

where  $T_{\text{ref}}$  is the reference temperature (K),  $T$  is the test temperature (K), and  $C_{1g}$  and  $C_{2g}$  are constants (17.44 and 51.6, respectively) (Nuñez et al. 2004; Tajvidi et al. 2005; Xu et al. 2010, 2011). Creep tests using the SIM were conducted at a reference temperature of 20 °C and isotherms between 20 and 75 °C at intervals of 5 °C. For each isotherm, 20% of the average breaking load (ABL) was applied for 2 h.

The construction of a master curve using the SSM involves shifting the timescale of the measured creep curves, and the creep strain at a reference stress is given by the following equation (Eq. 5):

$$\varepsilon(\sigma_r, t) = \varepsilon(\sigma, t / \alpha_\sigma) \quad (5)$$

where  $\varepsilon$  is the creep strain as a function of stress and time,  $\sigma_r$  is the reference stress,  $\sigma$  is the elevated stress, and  $\alpha_\sigma$  is the shift factor. The reference stress was 20% of the ABL, and the dwell time was 2 h for each isostress. Creep tests using the SSM were conducted at isostresses between 20 and 75% ABL at intervals of 5% ABL. In addition, different SSM testing parameters were used to investigate the differences between the SSM creep tests. The stepwise increases in stress were 5, 7.5, 10, and 12.5% ABL, and the dwell times were 2, 3, or 5 h. On the other hand, as shown in Eq. (6), the activation volume was calculated based on the Eyring model. This model is more suitable for the creep behavior of a polymer composite at temperatures below the  $T_g$  and was used to estimate the shift factor ( $\alpha_\sigma$ ), which shows the following express rate with the stress level (Giannopoulos and Burgoyne 2011; Hadid et al. 2014):

$$\log \alpha_\sigma = \log \left( \frac{\dot{\varepsilon}}{\dot{\varepsilon}_r} \right) = \frac{V^*}{2.30kT} (\sigma - \sigma_{\text{ref}}) \quad (6)$$

where  $\dot{\varepsilon}$  is the creep rate at the elevated stress ( $\sigma$ ),  $\dot{\varepsilon}_r$  is the creep rate at the reference stress ( $\sigma_{\text{ref}}$ ),  $V^*$  is the activation volume,  $k$  is Boltzmann constant, and  $T$  is the absolute temperature.

A full-scale experimental creep test was implemented to serve as a basis of comparison for the results of the accelerated creep tests. The applied stress was 20% of the ABL, and the mid-span deflection values of the samples were measured and recorded using a linear variable differential transducer (LDVT) for a period of 90 days. Three samples of each WPC were tested. All the samples during the accelerated and experimental creep tests were held at 20 °C and 65% RH.

## Analysis of variance

All the results are expressed as the mean  $\pm$  SD. The significance of the differences was calculated using Scheffe's test;  $p < 0.05$  was considered to be significant.

## Results and discussion

### Physical properties

The density, moisture content, water absorption, and thickness swelling of the WPCs are listed in Table 1. The density of each composite was approximately  $1000 \text{ kg/m}^3$ , indicating that there were no statistical significances ( $p > 0.05$ ) in density between the composites. It can be seen that the moisture contents of all the WPCs are the same (ca. 1.0%). This result indicated that the MAPP content does not influence the moisture content. In addition, water absorption and thickness swelling were measured after 24 h of soaking to estimate the dimensional stability of WPCs. The water absorption and thickness swelling of WPC<sub>0</sub> were 1.1 and 0.7%, respectively. It is well known that these characteristics of composites are attributed to several factors: (1) the influences of lumens, fine pores, and the hydrophilic nature of WFs due to the hydrogen bonding of water molecules to free hydrogen groups present in the cell wall, especially hemicelluloses (Ashori and Sheshmani 2010); (2) the gaps and flaws at the WFs–polymer matrix interface and microcracks in the polymer matrix, which are formed during composite processing (Espert et al. 2004; Adhikary et al. 2008); and (3) water diffusion blockage of higher density of composites that were subjected to high compression and filling during processing, which reduces their ability to absorb water (Clemons and Ibach 2004). Furthermore, the water absorption and thickness swelling of composites significantly decreased to 0.8 and 0.2% as the MAPP content increased up to 3 and 5 wt%, respectively. These results may be mainly explained by the improved interfacial bonding between the WFs and PP matrix due to the incorporation of MAPP, which can decrease the gaps and flaws at the WFs–polymer matrix interface and slow the water diffusion (Xie et al. 2010).

### Mechanical properties and impact strength

The flexural properties, wood screw holding strength, and impact strength of various WPCs are summarized in Table 1. It can be seen that the MOR of the WPCs increased markedly with increasing MAPP content up to 3 wt%, but beyond this point, it decreased gradually. A similar trend was also observed for the MOE. Thus, the results indicated that the WPC with 3 wt% MAPP exhibited the best flexural properties with MOR and MOE values of 33.5 MPa and 3.1 GPa, respectively. The improved flexural properties of WPCs with MAPP can be attributed to two factors. First, the anhydride groups in the MAPP react with the hydroxyl groups of the WFs to form ester bonds, which increase interfacial bonding between the PP matrix and WFs (Kazayawoko et al. 1997). Second is the improvement in the dispersion of WFs in PP matrix (Bledzki et al. 2005). However, by further increasing the MAPP content beyond 5 wt%, a significant decrease in MOR was observed. This phenomenon may be because the excess MAPP acts as a plasticizer, and it can be freely dispersed in the PP matrix (Bledzki et al. 2005). Furthermore, adding 1 wt% MAPP to the WPC caused a significant increase in the wood screw holding strength (from 1.1

to 1.8 kN), but beyond 1 wt%, it plateaus. Based on the abovementioned result, the improved interfacial bonding between the WFs and PP matrix increases the wood screw holding strength of the WPCs with MAPP, and this phenomenon was attributed to the increase in the ability of the WFs to conform around the thread of the screw, which could transfer the load continuously through the thread (Ayrilmis et al. 2011). However, in this study, the impact strengths of all the WPCs were in the range of 3.7–4.1 kN, indicating that there was no significant difference between the impact strengths of the WPCs with MAPPs and WPC<sub>0</sub>.

### Creep master curves using the SIM

This section outlines the use of the SIM for the accelerated creep tests in a range of elevated temperatures. Using WPC<sub>0</sub> as an example, Fig. 1a shows the flexural creep strain with increasing temperature over the actual time for the duration of the experiment. The master curve of the SIM was constructed by the following three steps of the test data adjustments: (1) rescaling, (2) eliminating the period before the onset time, and (3) horizontal shifting.

The rescaling and eliminating processes were carried out as the first two steps in the SIM. In this study, the rescaling and eliminating processes were conducted using a modified method described by Yeo and Hsuan (2009). As shown in Fig. 1b, a series of independent creep curves from stepwise sequential temperature increases were shifted to the reference temperature (20 °C) along the log scale of the time axis. In addition, the time before the onset of the creep strain for an individual curve is eliminated in Fig. 1c, which is the creep region that is most influenced by the temperature and history of heat. After rescaling and eliminating, the individual creep curves should be horizontally transited along the time axis to construct the master curve according to the shift factor,  $\log(\alpha_T)$ . For shorter times, the magnitude is a function of the elevated temperature and calculated from the WLF equation. The completely shifted master curve is shown in Fig. 1d. On the other hand, Fig. 1e shows the SIM master curves and the fitted curves for various WPCs. For the fitting curves, the creep master curves were fitted with an exponential growth equation with three parameters, which is given by the following equation:

$$S(t) = S_0 + ae^{bt} \quad (7)$$

where  $S(t)$  is the time-dependent compliance value,  $S_0$  is the instantaneous elastic compliance value,  $a$  and  $b$  are constant values, and  $t$  is the elapsed time. As shown in Fig. 1f, the model fits the SIM master curves very well, and the  $R^2$  values were greater than 0.99. However, the result revealed that the creep strain curves of the SIM were slightly higher than those of the experimental data (ED). This difference can be explained by two major reasons. First, the applied load leads to a stiffening of the material with increasing time in the experimental creep test, which is called physical aging (Brinson and Brinson 2008). Second, the WPCs undergo thermal expansion. Due to the overestimation of the creep strain by the SIM, the SSM was used to investigate and predict the long-term creep behavior of WRCs in the following section.

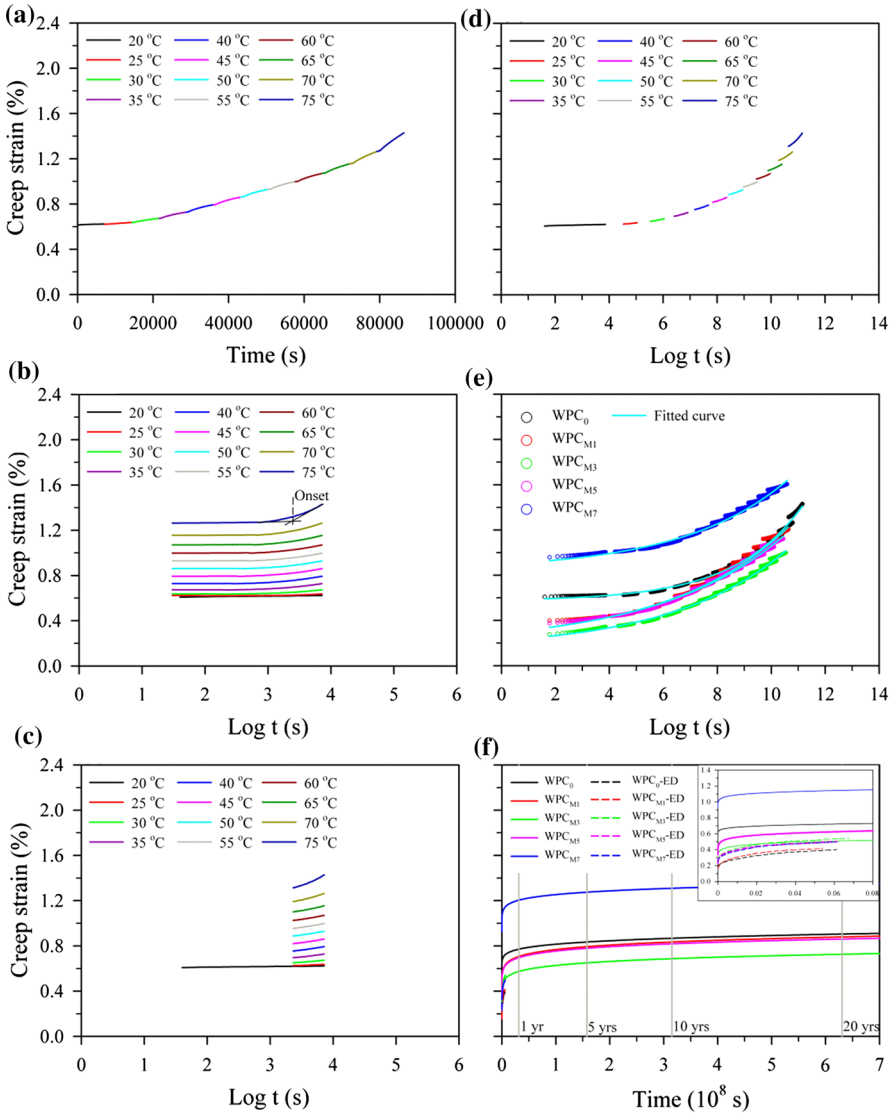


**Fig. 1** **a** SIM creep strain of the WPC<sub>0</sub> (reference temperature 20 °C; interval temperature 5 °C; dwelling time 2 h). Processing of the test data of the SIM method for WPC<sub>0</sub>: **b** rescaled creep curves, **c** eliminating the period before the onset time of each stress step, and **d** horizontal shifting. **e** SIM creep curves and fit curves for WPCs. **f** Comparison of the experimental data (ED) and fitted curves

**Creep master curves using the SSM**

Unlike the SIM, the SSM requires performing four adjustment steps (vertical shifting, rescaling, eliminating, and horizontal shifting) on the test data to produce the master curve. Figure 2a shows the SSM creep curve of WPC<sub>0</sub>, which

was constructed using the loading sequence of the SSM testing procedure at a reference stress of 20% ABL with a 5% stepwise increase in ABL and a dwelling time of 5 h. An immediate strain jump between the load steps was observed in

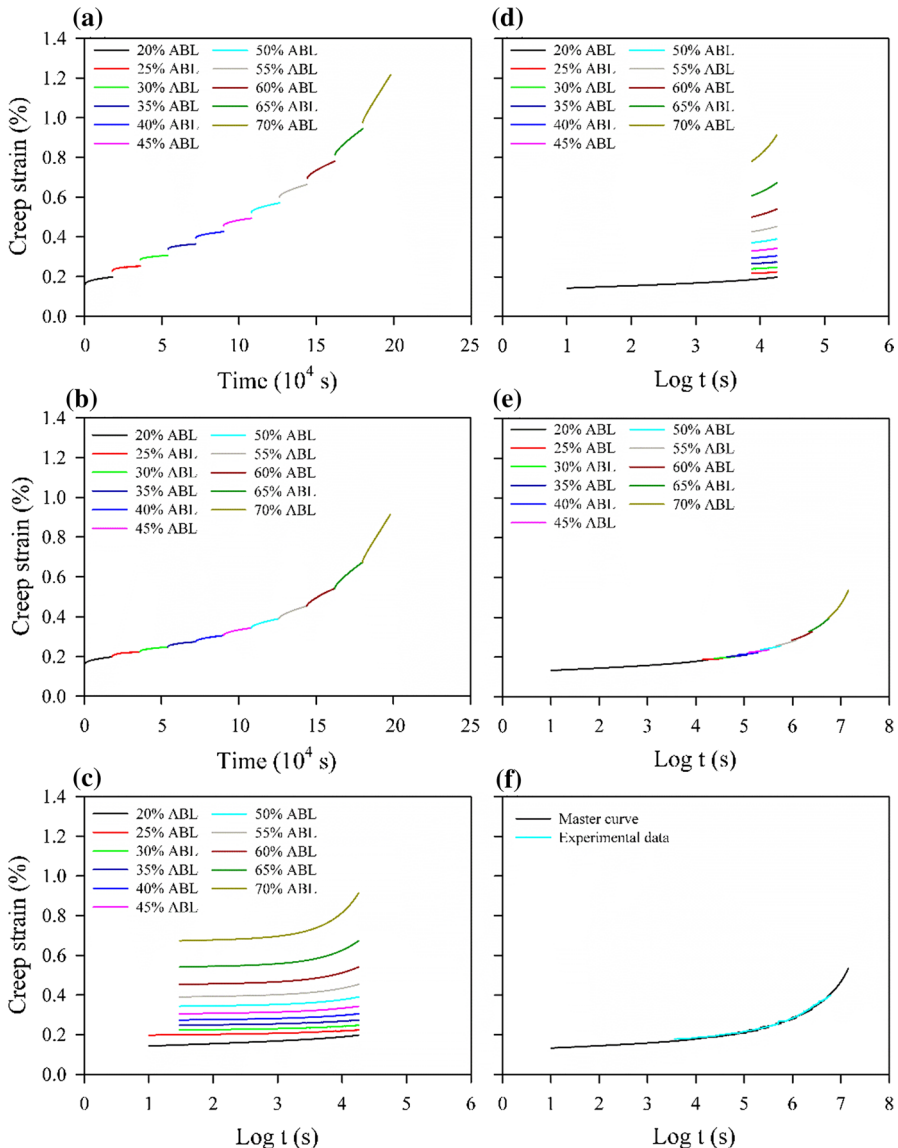


**Fig. 2** a SSM creep strain of the WPC<sub>0</sub> (reference stress 20% ABL; interval stress 5% ABL; dwelling time 5 h). Processing of the test data of the SSM method for WPC<sub>0</sub>; b vertical shifting, c rescaled creep curves, d eliminating the period before the onset time of each stress step, and e horizontal shifting. f Experimental data and master curve

the SSM creep curve. These jumps are subtracted by vertical shifting to eliminate the elastic component in the recorded strain, and there was no creep strain at each jump since the composites are elastic under instantaneous strain. Through this shifting process, at each load step, the start of the current curve was linked to the end of the previous curve to generate the continuous creep strain curve shown in Fig. 2b.

The rescaling step for the SSM accounted for the deformation and damage from previous steps because of the stress and strain history. Several rescaling operations were proposed by previous studies, such as a purely graphic approach (Giannopoulos and Burgoyne 2011), a power-law fit (Hadid et al. 2014), and a Prony series fit (Tanks et al. 2017). In this study, this approach was carried out by the modified method that was recommended by Yeo and Hsuan (2009). A series of independent creep curves were shifted to the reference stress level, as shown in Fig. 2c. The time before the onset time at the primary creep region, which is influenced by the stress level and history of the creep strain, was eliminated from the individual curves (Fig. 2d). As a result of the elimination, according to the shift factor,  $\log(\alpha_\sigma)$ , which is a function of the stress level, the master curve was constructed from horizontal shifting of the individual creep curves along the time axis. Figure 2e illustrates the final smooth master curve of WPC<sub>0</sub> obtained after the SSM processing steps described above. Finally, as shown in Fig. 2f, the SSM-fitted curve was well consistent with the long-term experimental data. These results demonstrated that the predicted creep curves of the WPCs using the SSM procedure were valid for matching the experimental data and worked better than the SIM procedure. Hadid et al. (2014) reported that the use of the SSM for polymer composites has two advantages over the SIM. One is that the properties of the materials are not influenced by temperature because the temperature is held constant. The other is the ability to prevent non-uniform heating of thick polymeric materials that have low thermal conductivity.

Furthermore, the effects of using different stress increments and dwelling time variations on the SSM master curves and the experimental data for WPC<sub>0</sub> and WPCs with various MAPP contents are shown in Fig. 3. The results showed that the master curve was not influenced by the test conditions for a given WPC sample, and these curves were highly consistent with the long-term creep behavior. Additionally, for a given set of test conditions, the data corresponding to the sample that failed during the jump to the final load step after a certain time were ignored. The shift factor is shown as a function of stress level in Fig. 4. It can be seen that a linear regression was performed to determine the slope of the plot of the shift factor versus the stress level, as validated by values of the coefficient of determination ( $R^2$ ) > 0.9. This result indicated that the superposition method used in conjunction with the SSM with different test conditions was validated to produce the creep master curve, indicating that the same creep mechanism was active. The activation volume ( $V^*$ ) was calculated from the linear slope of the plot of  $\log(\alpha_\sigma)$  versus  $(\sigma - \sigma_{\text{ref}})$  using the Eyring model shown in Eq. (6). Accordingly, the  $V^*$  of WPC<sub>0</sub> (2.94 nm<sup>3</sup>) was markedly higher than that of WPCs with various MAPP contents (1.30–1.40 nm<sup>3</sup>).

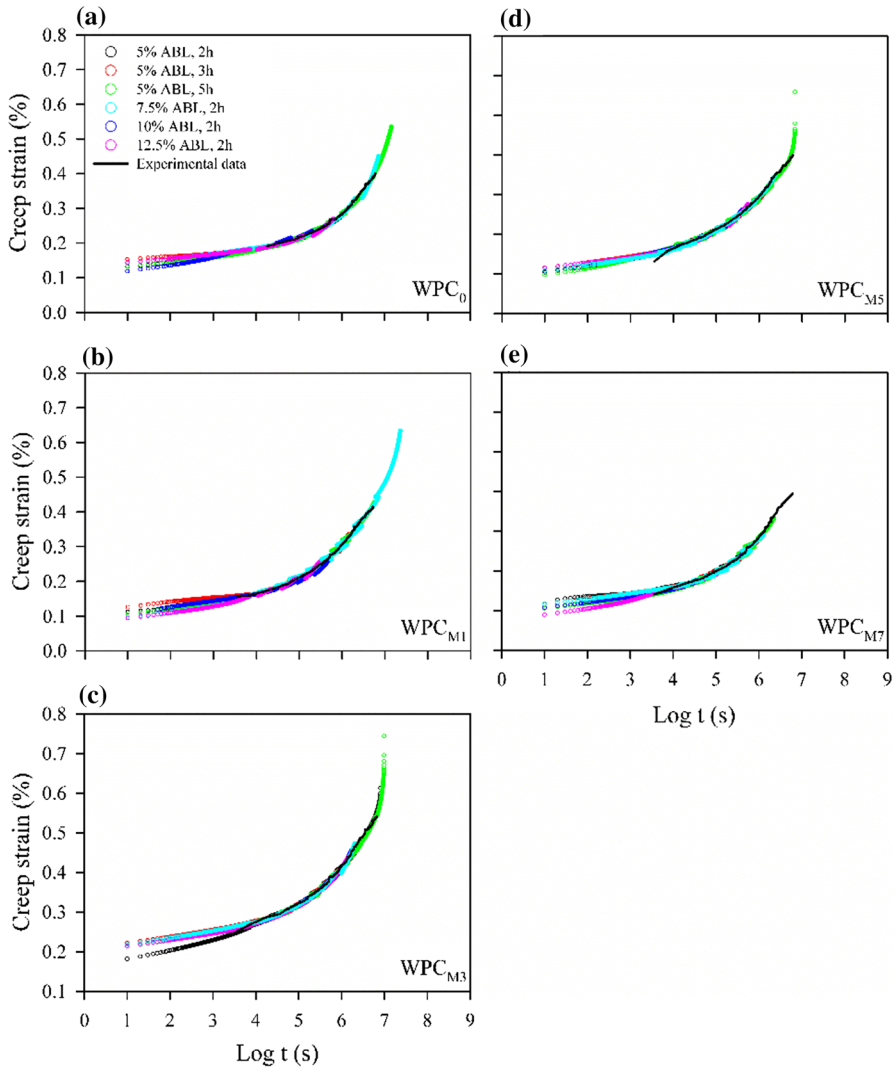


**Fig. 3** Master curves of the WPCs from different SSM testing parameters. **a** WPC<sub>0</sub>, **b** WPC<sub>M1</sub>, **c** WPC<sub>M3</sub>, **d** WPC<sub>M5</sub>, and **e** WPC<sub>M7</sub>

### SSM-predicted creep curves

The SSM-predicted compliance master curves of WPC<sub>0</sub> and WPCs with various MAPP contents on a log time scale are shown in Fig. 5a. It can be seen that all the WPCs with MAPP had lower creep compliance during the creep duration. Therefore, the WPCs with MAPP caused better creep resistance. In other words, the WPCs with MAPP showed a decrease in creep strain compared to the WPC without MAPP. The improvement in the creep resistance can be attributed to the

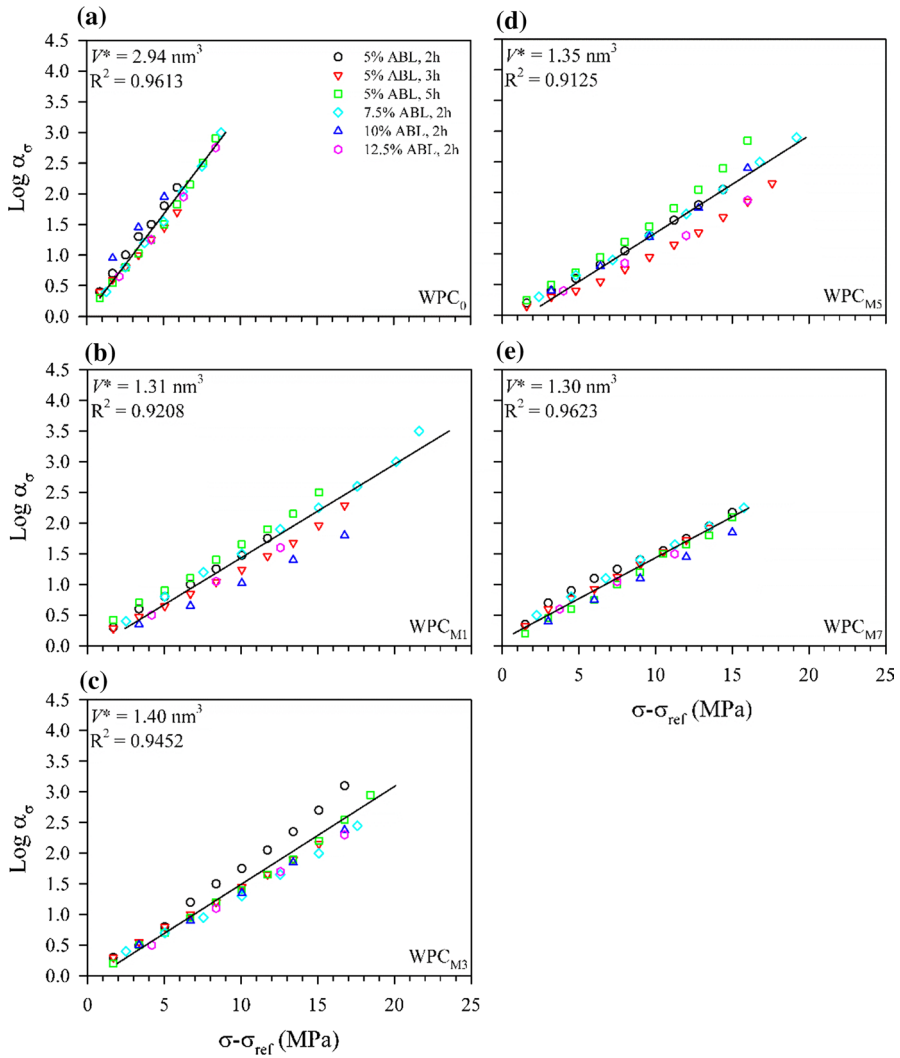


**Fig. 4** Relationships between the time–stress shift factor and stress level of the WPCs from different SSM testing parameters. **a** WPC<sub>0</sub>, **b** WPC<sub>M1</sub>, **c** WPC<sub>M3</sub>, **d** WPC<sub>M5</sub>, and **e** WPC<sub>M7</sub>

uniform dispersion of the WFs in the PP matrix and the increased interfacial bonding, which restrains the motion of polymer molecules in the interfacial layer (Bledzki and Faruk 2004; Acha et al. 2007; Gao et al. 2012). The fitted parameters of the exponential growth model (Eq. 7) are shown in Table 2, and the  $R^2$  values for all the WPCs are greater than 0.99. As shown in Fig. 5a, the model fits all the SSM master curves very well over the entire period.

**Fig. 5** SSM-fitted creep curves of various WPCs on a log time scale (a) and normal time scale (b)

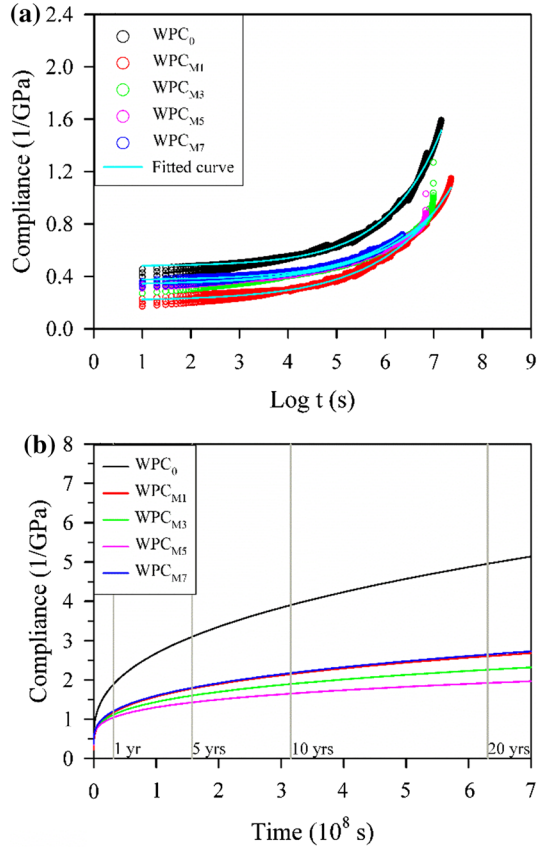


**Table 2** Fitted creep compliances of WPCs with different MAPP contents

Code	$S_0$ (1/GPa)	$a$	$b$	$R^2$	$S(t)$ (1/GPa)				ICR (%)			
					Time (years)				Time (years)			
					1	5	10	20	1	5	10	20
WPC <sub>0</sub>	0.48	$1.79 \times 10^{-3}$	0.89	0.9938	1.89	3.10	3.90	4.96	–	–	–	–
WPC <sub>M1</sub>	0.21	$4.92 \times 10^{-3}$	0.70	0.9954	1.17	1.78	2.15	2.60	38	43	45	47
WPC <sub>M3</sub>	0.34	$4.27 \times 10^{-3}$	0.69	0.9931	1.12	1.60	1.90	2.26	41	48	51	54
WPC <sub>M5</sub>	0.33	$6.88 \times 10^{-3}$	0.62	0.9957	1.04	1.43	1.65	1.92	45	54	58	61
WPC <sub>M7</sub>	0.37	$2.57 \times 10^{-3}$	0.77	0.9892	1.21	1.80	2.18	2.35	36	42	44	47

$S(t) = S_0 + ae^{bt}$ , where  $S(t)$  is the time-dependent compliance value,  $S_0$  is the instantaneous elastic compliance value, and  $a$  and  $b$  are constant values

On the other hand, Fig. 5b presents the SSM-fitted creep curves of all the WPCs on a normal time scale. As shown in Table 2, among the equation parameters, the WPCs with MAPP exhibited lower  $S_0$  values than WPC<sub>0</sub> (0.48 GPa<sup>-1</sup>). For the

fitting compliance,  $WPC_0$  showed 1.89, 3.10, 3.90, and 4.96  $\text{GPa}^{-1}$  at 1, 5, 10, and 20 years, respectively. When 1 wt% MAPP was added to the WPC, the compliance values of the resulting composite significantly declined to 1.17, 1.78, 2.15, and 2.60  $\text{GPa}^{-1}$  at 1, 5, 10, and 20 years, respectively. Similar trends were also observed for other WPCs with different MAPP contents, and their compliances decreased with increasing MAPP content up to 5 wt%. In other words, among all the WPCs, the compliance of  $WPC_{M5}$  was the lowest during the creep duration. In addition,  $WPC_{M5}$  showed the lowest  $b$  value (0.62), indicating it had the lowest creep rate and the highest creep resistance. However, when 7 wt% MAPP was added to the WPC, the sample's compliance increased to values similar to those of  $WPC_{M1}$ . This phenomenon is consistent with the results of MOR; the excess MAPP acts as a plasticizer due to its molecular weight being substantially lower than that of the matrix (Bledzki et al. 2005).

Furthermore, the improvement in the creep resistance (ICR) was calculated to estimate the creep resistance of the WPCs under long-term conditions, and the resistance is described by the following equation (Eq. 8):

$$\text{ICR} (\%) = \left[ 1 - \frac{S(t)_M}{S(t)_N} \right] \times 100 \quad (8)$$

where  $S(t)_M$  and  $S(t)_N$  are the time-dependent compliance with and without MAPP, respectively. As listed in Table 2, in addition to the ICR value increase with increasing creep time, the creep resistances of all WPCs with MAPP were significantly improved in the range of 47–61% over 20 years. Accordingly, these results demonstrated that the creep resistance of the WPC would be improved by the addition of an adequate amount of MAPP. Of these,  $WPC_{M5}$  exhibited the highest ICR value (61%), while  $WPC_{M1}$  and  $WPC_{M7}$  exhibited the smallest value (47%).

## Conclusion

MAPP exhibited excellent reinforcing effects on the physico-mechanical and creep properties of WPCs. The results showed that the water absorption and thickness swelling decreased with increasing MAPP content, whereas the flexural properties and wood screw holding strength were enhanced as the MAPP content was increased by up to 3 and 1 wt%, respectively. However, the MOR declined when the MAPP content exceeded 5 wt%. In addition, the SIM and SSM were used in this study to predict the long-term creep behavior of WPCs. The results indicated that the SSM was more suitable for constructing the master curve than the SIM, and the  $WPC_{M5}$  exhibited the best creep resistance among all the WPCs. The improvements in these properties in the composites can be attributed to the increased interfacial interactions between the wood fibers and polymer matrix, which play a role in stress transition. Accordingly, the addition of an adequate amount of MAPP to the WPC can improve not only its mechanical performance but also its creep resistance, especially with 3–5 wt% MAPP. In addition, the results of this study provided a reliable SSM approach for predicting the long-term creep behavior for WPCs.

**Acknowledgements** This work was financially supported by a Research Grant from the Ministry of Science and Technology, Taiwan (MOST 105-2628-B-005-002-MY3).

## References

- Acha BA, Reboredo MM, Marcovich NE (2007) Creep and dynamic mechanical behavior of PP-jute composites: effect of the interfacial adhesion. *Compos Part A* 38:1507–1516. <https://doi.org/10.1016/j.compositesa.2007.01.003>
- Achereiner F, Engelsing K, Bastian M, Heidemeyer P (2013) Accelerated creep testing of polymers using the stepped isothermal method. *Polym Test* 32:447–454. <https://doi.org/10.1016/j.polymertesting.2013.01.014>
- Adhikary KB, Pang S, Staiger MP (2008) Dimensional stability and mechanical behavior of wood–plastic composites based on recycled and virgin high-density polyethylene (HDPE). *Compos Part B* 39:807–815. <https://doi.org/10.1016/j.compositesb.2007.10.005>
- Alwis KGNC, Burgoyne CJ (2008) Accelerated creep testing for aramid fibres using the stepped isothermal method. *J Mater Sci* 43:4789–4800. <https://doi.org/10.1007/s10853-008-2676-0>
- Ashori A, Sheshmani S (2010) Hybrid composites made from recycled materials: moisture absorption and thickness swelling behavior. *Bioresour Technol* 101:4717–4720. <https://doi.org/10.1016/j.biortech.2010.01.060>
- Ayrlimis N, Jarusombuti S, Fueangvivat V, Bauchongkol P (2011) Effect of thermal-treatment of wood fibers on properties of flat-pressed wood plastic composites. *Polym Degrad Stab* 96:818–822. <https://doi.org/10.1016/j.polymdegradstab.2011.02.005>
- Bledzki AK, Faruk O (2004) Creep and impact properties of wood fibre–polypropylene composites: influence of temperature and moisture content. *Compos Sci Technol* 64:693–700. [https://doi.org/10.1016/S0266-3538\(03\)00291-4](https://doi.org/10.1016/S0266-3538(03)00291-4)
- Bledzki AK, Letman M, Viksne A, Rence L (2005) A comparison of compounding processes and wood type for wood fibre-PP composites. *Compos Part A* 36:789–797. <https://doi.org/10.1016/j.compositesa.2004.10.029>
- Brinson HF, Brinson LC (2008) *Polymer engineering science and viscoelasticity, an introduction*. Springer, New York
- Clemons CM, Ibach RE (2004) Effects of processing method and moisture history on laboratory fungal resistance of wood–HDPE composites. *Forest Prod J* 54:50–57. <https://www.fs.usda.gov/treesearch/pubs/6355>
- Das M, Chakraborty D (2008) Evaluation of improvement of physical and mechanical properties of bamboo fibres due to alkali treatment. *J Appl Polym Sci* 107:522–527. <https://doi.org/10.1002/app.26155>
- Dasappa P, Lee-Sullivan P, Xiao X (2009) Temperature effects on creep behavior of continuous fiber GMT composites. *Compos Part A* 40:1071–1081. <https://doi.org/10.1016/j.compositesa.2009.04.026>
- Dittenber DB, Ganga Rao HVS (2012) Critical review of recent publications on use of natural composites in infrastructure. *Compos Part A* 43:1419–1429. <https://doi.org/10.1016/j.compositesa.2011.11.019>
- Espert A, Vilaplana F, Karlsson S (2004) Comparison of water absorption in natural cellulosic fibres from wood and one-year crops in polypropylene composites and its influence on their mechanical properties. *Compos Part A* 35:1267–1276. <https://doi.org/10.1016/j.compositesa.2004.04.004>
- Felix JM, Gatlenholm P (1991) The nature of adhesion in composites of modified cellulose fibers and polypropylene. *J Appl Polym Sci* 42:609–620. <https://doi.org/10.1002/app.1991.070420307>
- Gao H, Xie Y, Ou R, Wang Q (2012) Grafting effects of polypropylene blends with maleic anhydride on the properties of the resulting wood-plastic composites. *Compos Part A* 43:150–157. <https://doi.org/10.1016/j.compositesa.2011.10.001>
- Giannopoulos IP, Burgoyne CJ (2011) Prediction of the long-term behaviour of high modulus fibres using the stepped isostress method (SSM). *J Mater Sci* 46:7660–7671. <https://doi.org/10.1007/s10853-011-5743-x>
- Giannopoulos IP, Burgoyne CJ (2012) Accelerated and real-time creep and creep-rupture results for aramid fibers. *J Appl Polym Sci* 125:3856–3870. <https://doi.org/10.1002/app.36707>

- Hadid M, Rechak S, Tati A (2004) Long-term bending creep behavior prediction of injection molded composite using stress-time correspondence principle. *Mater Sci Eng, A* 385:54–58. <https://doi.org/10.1016/j.msea.2004.04.023>
- Hadid M, Guerira B, Bahri M, Zouani A (2014) Assessment of the stepped isostress method in the prediction of long term creep of thermoplastics. *Polym Testing* 34:113–119. <https://doi.org/10.1016/j.polymertesting.2014.01.003>
- Hung KC, Wu JH (2010) Mechanical and interfacial properties of plastic composite panels made from esterified bamboo particles. *J Wood Sci* 56:216–221. <https://doi.org/10.1007/s10086-009-1090-9>
- Hung KC, Wu TL, Chen YL, Wu JH (2015) Assessing the effect of wood acetylation on mechanical properties and extended creep behavior of wood/recycled-polypropylene composites. *Constr Build Mater* 108:139–145. <https://doi.org/10.1016/j.conbuildmat.2016.01.039>
- Jones CJFP, Clarke D (2007) The residual strength of geosynthetic reinforcement subjected to accelerated creep testing and simulated seismic events. *Geotext Geomembr* 25:155–169. <https://doi.org/10.1016/j.geotexmem.2006.12.004>
- Kazayawoko M, Balatinez JJ, Woodhams RT (1997) Diffuse reflectance Fourier transform infrared spectra of wood fibers treated with maleated polypropylenes. *J Appl Polym Sci* 66:1163–1173. [https://doi.org/10.1002/\(SICI\)1097-4628\(19971107\)66:6%3C1163::AID-APP16%3E3.0.CO;2-2](https://doi.org/10.1002/(SICI)1097-4628(19971107)66:6%3C1163::AID-APP16%3E3.0.CO;2-2)
- Keener TJ, Stuart RK, Brown TK (2004) Maleated coupling agents for natural fibre composites. *Compos Part A* 35:357–362. <https://doi.org/10.1016/j.compositesa.2003.09.014>
- Klyosov A (2007) Wood–plastic composites. Wiley, Hoboken
- Kumar V, Tyagi L, Sinha S (2011) Wood flour–reinforced plastic composites: a review. *Rev Chem Eng* 27:253–264. <https://doi.org/10.1515/REVCE.2011.006>
- Lee CH, Wu TL, Chen YL, Wu JH (2010) Characteristics and discrimination of five types of wood–plastic composites by Fourier transform infrared spectroscopy combined with principal component analysis. *Holzforschung* 64:699–704. <https://doi.org/10.1515/HF.2010.104>
- Li X, Tabil LG, Panigrahi S (2007) Chemical treatments of natural fiber for use in natural fiber-reinforced composite: a review. *J Polym Environ* 15:25–33. <https://doi.org/10.1007/s10924-006-0042-3>
- Liu H, Wu Q, Han G, Yao F, Kojima Y, Suzuki S (2008) Compatibilizing and toughening bamboo flour-filled HDPE composites: mechanical properties and morphologies. *Compos Part A* 39:1891–1900. <https://doi.org/10.1016/j.compositesa.2008.09.011>
- Mishra S, Naik JB, Patil YP (2000) The compatibilizing effect of maleic anhydride on swelling and mechanical properties of plant-fiber-reinforced novolac composites. *Compos Sci Technol* 60:1729–1735. [https://doi.org/10.1016/S0266-3538\(00\)00056-7](https://doi.org/10.1016/S0266-3538(00)00056-7)
- Mohanty S, Nayak SK, Verma SK, Tripathy SS (2004) Effect of MAPP as a coupling agent on the performance of jute-PP composites. *J Reinf Plast Comp* 23:625–637. <https://doi.org/10.1177/0731684404032868>
- Núñez AJ, Marcovich NE, Aranguren MI (2004) Analysis of the creep behavior of polypropylene–wood flour composites. *Polym Eng Sci* 44:1594–1603. <https://doi.org/10.1002/pen.20157>
- Oksman K, Skrifvars M, Selin JF (2003) Natural fibres as reinforcement in polylactic acid (PLA) composites. *Compos Sci Technol* 63:1317–1324. [https://doi.org/10.1016/S0266-3538\(03\)00103-9](https://doi.org/10.1016/S0266-3538(03)00103-9)
- Ou R, Zhao H, Sui S, Song Y, Wang Q (2010) Reinforcing effects of Kevlar fiber on the mechanical properties of wood-flour/high-density-polyethylene composites. *Compos Part A* 41:1272–1278. <https://doi.org/10.1016/j.compositesa.2010.05.011>
- Pelaez-Samaniego MR, Yadama V, Lowell E, Espinoza-Herrera R (2013) A review of wood thermal pre-treatments to improve wood composite properties. *Wood Sci Technol* 47:1285–1319. <https://doi.org/10.1007/s00226-013-0574-3>
- Qiu W, Zhang F, Endo T, Hirotsu T (2003) Preparation and characteristics of composites of high-crystalline cellulose with polypropylene: effects of maleated polypropylene and cellulose content. *J Appl Polym Sci* 87:337–345. <https://doi.org/10.1002/app.11446>
- Rowell RM (1983) Chemical modification of wood. *For Prod Abstr* 6:363–382
- Saba N, Paridah MT, Jawaid M (2015) Mechanical properties of kenaf fibre reinforced polymer composite: a review. *Constr Build Mater* 76:87–96. <https://doi.org/10.1016/j.conbuildmat.2014.11.043>
- Schneider MH, Vasic S, Lande S, Phillips JG (2003) Static bending and toughness of wood polymer composites (yellow birch and basswood). *Wood Sci Technol* 37:165–176. <https://doi.org/10.1007/s00226-003-0189-1>
- Tajvidi M, Falk RH, Hermanson JC (2005) Time-temperature superposition principle applied to a kenaf fiber/high density polyethylene composites. *J Appl Polym Sci* 97:1995–2004. <https://doi.org/10.1002/app.21648>

- Tanks JD, Rader KE, Sharp SR (2017) Accelerated creep and creep-rupture testing of transverse unidirectional carbon/epoxy lamina based on the stepped isostress method. *Compos Struct* 159:455–462. <https://doi.org/10.1016/j.compstruct.2016.09.096>
- Xie Y, Xiao Z, Grüneberg T, Militz H, Hill CAS, Steuernagel L, Mai C (2010) Effects of chemical modification of wood particles with glutaraldehyde and 1,3-dimethylol-4,5-dihydroxyethyleneurea on properties of the resulting polypropylene composites. *Compos Sci Technol* 70:2003–2011. <https://doi.org/10.1016/j.compscitech.2010.07.024>
- Xu B, Simonsen J, Rochefort WE (2001) Creep resistance of wood-filled polystyrene/high-density polyethylene blends. *J Appl Polym Sci* 79:418–425. [https://doi.org/10.1002/1097-4628\(2001118\)79:3%3C418::AID-APP40%3E3.0.CO;2-X](https://doi.org/10.1002/1097-4628(2001118)79:3%3C418::AID-APP40%3E3.0.CO;2-X)
- Xu Y, Wu Q, Lei Y, Yao F (2010) Creep behavior of bagasse fiber reinforced polymer composites. *Biore-sour Technol* 101:3280–3286. <https://doi.org/10.1016/j.biortech.2009.12.072>
- Xu Y, Lee SY, Wu Q (2011) Creep analysis of bamboo high-density polyethylene composites: effect of interfacial treatment and fiber loading level. *Polym Compos* 32:692–699. <https://doi.org/10.1002/pc.21088>
- Yang TC, Wu TL, Hung KC, Chen YL, Wu JH (2015) Mechanical properties and extended creep behavior of bamboo fiber reinforced recycled poly(lactic acid) composites using the time-temperature superposition principle. *Constr Build Master* 93:558–563. <https://doi.org/10.1016/j.conbuildmat.2015.06.038>
- Yeo SS, Hsuan YG (2009) Predicting the creep behavior of high density polyethylene geogrid using stepped isothermal method. In: Martin JW, Ryntz RA, Chin J, Dickie RA (eds) *Service life prediction of polymeric materials: global perspectives*. Springer, New York, pp 205–218
- Yeo SS, Hsuan YG (2010) Evaluation of creep behavior of high density polyethylene and polyethylene-terephthalate geogrids. *Geotext Geomembr* 28:409–421. <https://doi.org/10.1016/j.geotextmem.2009.12.003>
- Zhang F, Endo T, Qiu W, Yang L, Hirotsu T (2002) Preparation and mechanical properties of composite of fiPrepa cellulose and maleated polyethylene. *J Appl Polym Sci* 84:1971–1980. <https://doi.org/10.1002/app.10428>

**Publisher's Note** Springer Nature remains neutral with regard to jurisdictional claims in published maps and institutional affiliations.